


Recent Advancements in Retinal Vessel Segmentation

Chetan L Srinidhi¹  · P Aparna¹ · Jeny Rajan²

Received: 6 January 2017 / Accepted: 1 March 2017
© Springer Science+Business Media New York 2017

Abstract Retinal vessel segmentation is a key step towards the accurate visualization, diagnosis, early treatment and surgery planning of ocular diseases. For the last two decades, a tremendous amount of research has been dedicated in developing automated methods for segmentation of blood vessels from retinal fundus images. Despite the fact, segmentation of retinal vessels still remains a challenging task due to the presence of abnormalities, varying size and shape of the vessels, non-uniform illumination and anatomical variability between subjects. In this paper, we carry out a systematic review of the most recent advancements in retinal vessel segmentation methods published in last five years. The objectives of this study are as follows: first, we discuss the most crucial preprocessing steps that are involved in accurate segmentation of vessels. Second, we review most recent state-of-the-art retinal vessel segmentation techniques which are classified into different categories based on their main principle. Third, we quantitatively analyse these methods in terms of its sensitivity, specificity,

accuracy, area under the curve and discuss newly introduced performance metrics in current literature. Fourth, we discuss the advantages and limitations of the existing segmentation techniques. Finally, we provide an insight into active problems and possible future directions towards building successful computer-aided diagnostic system.

Keywords Review · Retinal vessel · Segmentation · Fundus image

Introduction

Retinal diseases are of the most significant public health concern in the working and aged population across worldwide. For instance, Diabetic Retinopathy (DR), Glaucoma and Age-related Macular Degeneration (AMD) are the leading causes of blindness in the ageing population [1–3]. In a recent study [1], it is estimated that there are 93 million people with DR followed by AMD which accounts for 7–8 % of total blindness worldwide [2]. Another major leading cause of blindness is the Glaucoma, characterized by progressive damage to the optic nerve. It is estimated that there are about 64.3 million people with Glaucoma [3]. All these retinal diseases are likely to increase by three folds as a consequence of exponential ageing population, diabetes, lifestyle changes, and other risk factors. Such statistics naturally drives a considerable amount of research dedicated in developing computer-aided diagnostic (CAD) tool for the automated diagnosis of retinal pathologies, mainly for low and middle-income countries.

The segmentation of retinal vessels is particularly important for diagnosis assistance, treatment and surgery planning of retinal diseases. Retinal vessel segmentation is indeed a fundamental step in the accurate visualization and

This article is part of the Topical Collection on *Image & Signal Processing*

✉ Chetan L Srinidhi
srinidhipy@gmail.com
Aparna P
p.aparnadinesh@gmail.com
Jeny Rajan
jenyrajan@gmail.com

¹ Department of Electronics and Communication Engineering, National Institute of Technology Karnataka, Surathkal, India

² Department of Computer Science and Engineering, National Institute of Technology Karnataka, Surathkal, India

quantification of retinal pathologies. Changes in vessel morphology such as shape, tortuosity, branching pattern and width provide an accurate early detection of many retinal diseases [4]. Clinically, retinal fundus images are often routinely acquired for mass screening of various abnormalities. Manual segmentation of vessel structures from these fundus images is often tedious, time-consuming and error-prone, especially for large population screening. Therefore, there is a need for the CAD tool which can reduce the number of manual operators with an increase in speed, accuracy, and reproducibility mainly for large population-based screening programs.

Over the past two decades, a tremendous amount of research has been devoted in segmenting the vessel structures from retinal fundus images. Numerous fully automated, semi-automated methods have been reported in the literature which were quite successful in achieving segmentation accuracy on par with trained human annotators. Despite this, there is a considerable scope for further improvements due to various challenges posed by the complex nature of vascular structures. Some of the active problems include segmentation in the presence of abnormalities, segmentation of thin vessel structures and segmentation near the bifurcation and crossover regions.

In this article, we considered retinal vessel segmentation methods published in the last five years. The primary objective of this study is to provide the readers with comprehensive insight on latest developments that has progressed over the last five years and highlighting the key design challenges that researchers may encounter in the development of new methods. The advancements in technological innovations in imaging modalities (like Fluorescence Angiography (FA), Scanning Laser Ophthalmoscope (SLO), Optical Coherence Tomography (OCT)) along with the combination of adaptive optics to FA, SLO and OCT has provided both spectacular spatial resolution as well as the depth information for clear visualization of anatomical components. In addition, standard acquisition protocol across different imaging devices have helped the research community to explore and validate their methods on more general and diverse datasets. Comprehensive and detailed survey of retinal vessel segmentation methods before this is published in [5].

The rest of the paper is organized as follows. In “[Retinal image processing](#)”, we provide a brief overview of different retinal imaging modalities, followed by the significance and existing challenges in retinal vessel segmentation. We present an overview of the articles published in the last five years along with their selection criteria in “[Methodology of the review](#)”. The image pre-processing steps generally employed before vessel segmentation methods is detailed in “[Image pre-preprocessing](#)”. The different categories of vessel segmentation methods are described in detail in

“[Segmentation methods](#)” along with their pros and cons. Subsequently, the summary of the recent state-of-the-art segmentation methods with the focus on existing segmentation challenges is presented in “[Summary of vessel segmentation methods](#)”. A brief overview of publicly available retinal image datasets, followed by the validation measures employed and thorough assessment of segmentation methods is presented in “[Review of validation](#)”. A general discussion on recapitulating the main points and future trends in retinal vessel segmentation are discussed in “[Discussion](#)”. Finally, the conclusions are drawn in “[Conclusions](#)”.

Retinal image processing

Imaging the retina is of prime importance for early diagnosis, monitoring disease progression, treatment and surgery planning of various retinal diseases. The retina is the most important part of the eye, which is formed by a thin layer of photosensitive neural cells which lies at the back (i.e. the fundus) of the eye. The image of the retina is acquired using specialized microscope attached with a camera called fundus camera. The fundus is the interior surface of the eye including the retina, optic disc, macula, and fovea. A typical human fundus photograph captured from the fundus camera is shown in Fig. 1. The microstructures present in the retina are the optic disc, macula and blood vessels such as arteries and veins.

The fundus photography is obtained by a projection of 3-D retinal tissue onto the 2-D imaging plane using reflected light. Among the different imaging modalities as shown in Fig. 2, the color fundus photography, FA and SLO images, are the most widely used imaging techniques for segmentation of retinal vessels. Fluorescein angiography is a process of imaging vascular flow within the retina and surrounding tissue by injecting a fluorescent dye into the blood

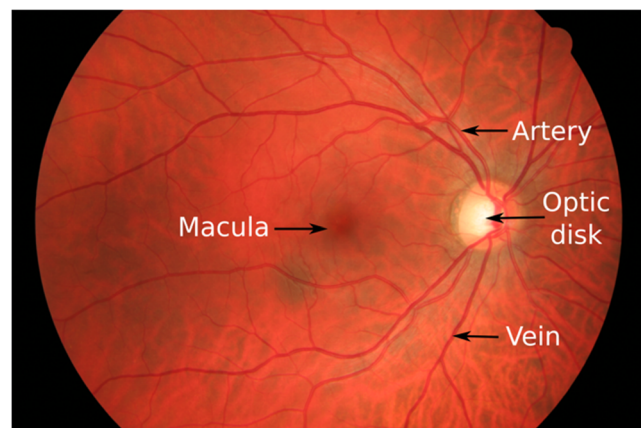
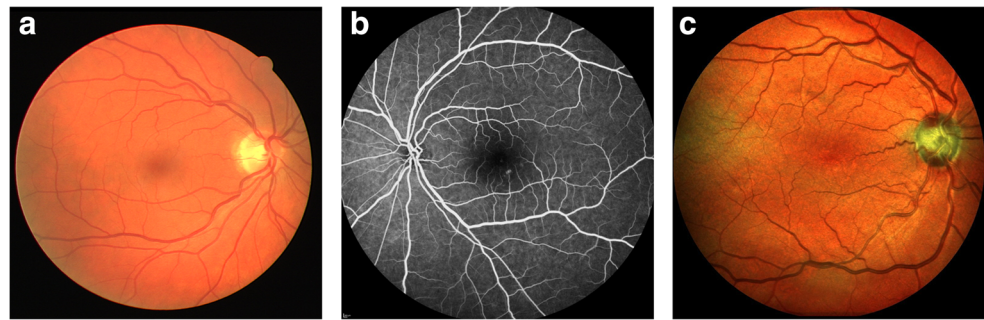


Fig. 1 A color fundus photograph of the retina from HRF dataset [91]

Fig. 2 Retinal imaging modalities. **a** The color fundus photography from DRIVE. [88] **b** Fluorescein Angiography (FA). [100] **c** Scanning Laser Ophthalmoscope (SLO) from IOSTAR. [97]



stream. This dye fluoresces a different color when light from a particular wavelength reaches it [4]. Recently, some of the researchers have made an attempt to evaluate the segmentation performance on FA [6] and SLO [101] images. Compared to fundus imaging, SLO has the advantages of lower levels of light exposure, direct digital imaging, provides very high contrast and finely detailed low resolution images (1K-1.5K pixels).

Need for retinal vessel segmentation

Retina is the only part of the human body that allows direct non-invasive visualization of its anatomical components. Many large-scale population-based studies [7–12] have been conducted to find statistical correlations between a disease and structural changes in the vascular system of the retina. Such studies have shown a strong relationship between retinal vasculature with number of conditions like hypertension [13, 14], stroke [8, 12], and cardiovascular diseases [10]. The segmentation of retinal vessels is a crucial task in automated early detection of these pathologies.

The key motivations which necessitate segmentation of retinal vasculature are listed below:

- One of the major landmark study conducted in [1], has shown a strong link between diabetic retinopathy and structural changes in retinal vasculature. The earliest sign of DR is the presence of tiny capillary dilations called microaneurysms usually appearing near thin vessels as shown in Fig. 3a. Although the segmentation of vasculature has no direct role in the assessment of these pathologies, it is necessary as pathological structures (such as microaneurysm, exudates) have similar visual features as high-curvature and junction points of thin vessels [45]. The knowledge of shape and characteristic of the retinal vasculature can also aid in accurate localization of other degenerative anatomical structures like the optic disc or macula [15].
- The Proliferative Diabetic Retinopathy (PDR) [16] is an advanced stage of DR which is primarily characterized by abnormal growth of new blood vessels which is termed as neovascularization. The abnormal growth of

new vessels is triggered mainly to compensate for the damaged blood vessels caused by DR. The new blood vessels appear in loopy structures mainly near the optic disc region or the veins as shown in Fig. 3b. Since conventional vessel segmentation algorithms consider a vessel as a thin elongated smooth linearly varying structure, it often fails to detect complex structures like neovascularization (see Fig. 3b).

- Recent study in [17], has shown a link between Retinopathy of Prematurity (ROP) and the temporal changes of retinal vessel width and tortuosity. One of the earliest changes visible in vessel morphology is an increase in vessel tortuosity [19, 20] as depicted in Fig. 3c. The increase in vessel tortuosity has shown a link with the progression of ROP, hypertensive retinopathy [18], and some rarer hereditary retinopathies.
- The ratio of arteries to veins width (A/V ratio), arteriovenous (AV) nicking as depicted in Fig. 3d have shown to be associated with hypertension, cardiovascular and other systemic diseases [10–12, 102]. The Blue Mountains eye population-based study [9] proved the hypothesis that small vessel structural changes may precede the development of severe hypertension. The analysis of such retinal microvasculature requires precise tools to extract the vessel tree, quantify the morphological changes and evaluate the condition of the patients.

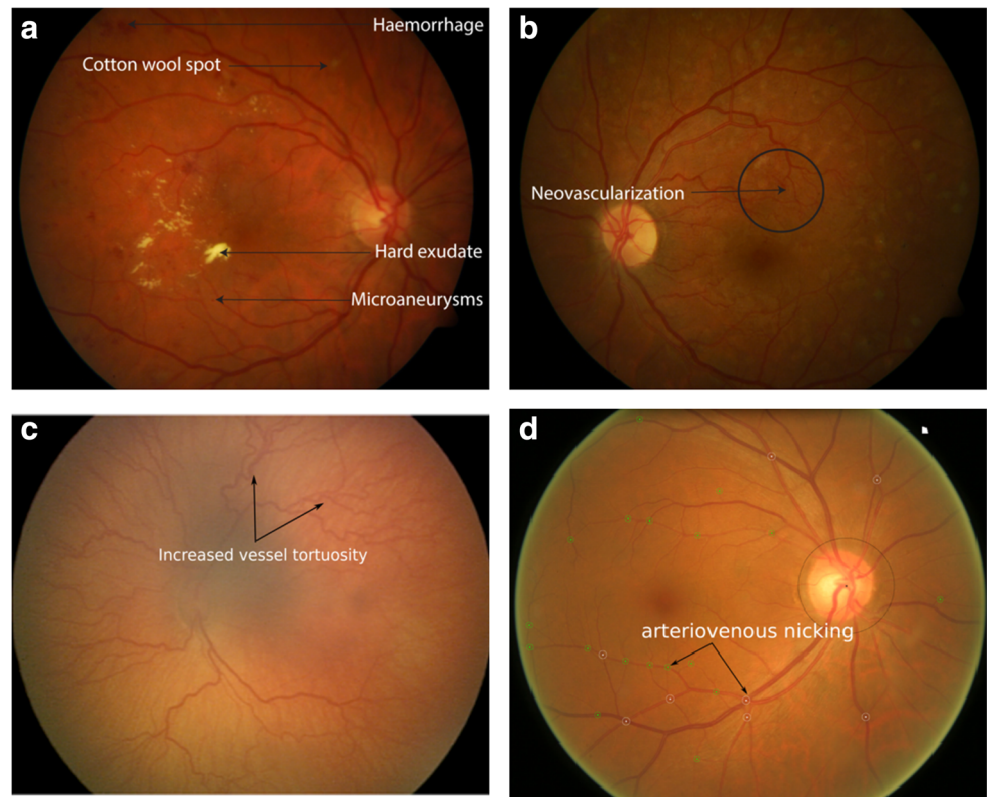
Challenges in retinal vessel segmentation

Many automated retinal vessel segmentation methods have been proposed in the literature. Although most of the existing methods have been successful in achieving performance close to the trained human observers, there still exists many significant challenges in clinical scenarios.

The following are some of the current challenges and open problems related to retinal vessel segmentation:

- During acquisition of retinal fundus images, different 3D retinal structures with varying depth are projected onto a 2D image with maximum intensity. This leads to the overlapping of non-vascular structures and decrease in the visibility of thin vessels in low-contrast imaging

Fig. 3 **a** common signs of DR [92]. **b** common sign of Proliferative DR (PDR) [92]. **c** common sign of ROP (from Oloumi et al. [103], with kind permission from Elsevier). **d** arteriovenous nicking [102]



as illustrated in Fig. 4a. Due to the use of low quality fundus camera, various imaging artefacts such as blur, noise, uneven illumination and inter-camera variability may also be introduced.

– The majority of the existing methods have mainly focused on segmenting major (large) vessel structures. Accurate extraction of minor (thin) vessel structures is still very challenging and an open problem (see third

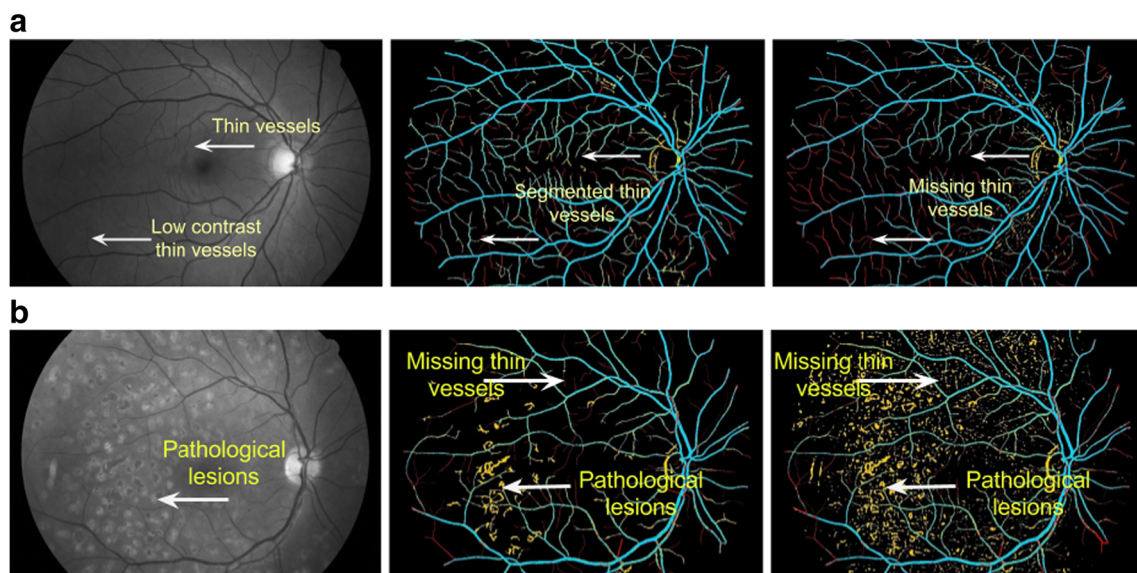


Fig. 4 Challenges in retinal vessel segmentation. Vessel segmentation in healthy image (*first row*) and DR image (*second row*). First column: original image; second column: segmentation result of the approach [73]; third column: segmentation result of MSLD method [24]. In the segmentation maps (*second, third column*), blue pixels

represent the true positives, red pixels are the false negatives, yellow pixels are the false positives, and black pixels are the true negatives. (Illustrations based on material from Christodoulidis et al. [73], with kind permission from Elsevier)

column Fig. 4a, b). Since large and small vessels differ in their size, shape, and contrast, they should be tackled differently because applying the same technique might tend to over segment the other.

- The presence of abnormalities such as exudates, haemorrhages, cotton wool spots and microaneurysms (see Fig. 4b), structures with strong central vessel reflex, bifurcations/crossover regions, close parallel and highly curved vessels (see Fig.5) pose a significant challenge for accurate segmentation of vessels.

Methodology of the review

In this review, we performed a comprehensive literature search on the recent retinal vessel segmentation techniques published in the last five years. A total of 56 peer-reviewed articles are listed in Table 1. were selected from the Google Scholar, PubMed and the Web of Science databases. The selection criteria include articles from peer-reviewed journals and conferences related to retinal vessel segmentation methods. The classification hierarchy is same as proposed in [5] to maintain the consistency and clarity for the sake of readers interested in carrying out research in this area.

Image pre-processing

Image pre-processing is an essential prerequisite for accurate segmentation of retinal vessels. Vessel segmentation is quite difficult due to various imaging conditions such as noise, intensity inhomogeneity, poor visibility of thin vessel structures, anatomical variations, and other imaging artefacts. These artefacts are often inherited mainly from the image acquisition process (because of low-quality

image acquisition devices). Thus, before applying any vessel segmentation techniques few preprocessing steps are applied to improve the segmentation accuracy. In general, there are three pre-processing steps involved before vessel segmentation.

- i) Removal of central vessel reflex
- ii) Intensity inhomogeneity correction
- iii) Vessel enhancement

These techniques don't necessarily guarantee to achieve higher segmentation accuracy. It totally depends on the developed method and application at hand. Therefore, the reader should be mindful about when and what pre-processing method to be employed for a given problem. All the preprocessing techniques have been experimented on the green channel of the RGB retinal image. This is because the green channel exhibits better contrast between the vessels and the background [21–25]. In [26], different color components were investigated and found that the green channel exhibits the highest contrast between vessels and background. Once the green channel is extracted from RGB retinal image the following preprocessing steps are performed.

Removal of central vessel reflex

Retinal vessels usually appear darker than the background surface because of lower reflectance. It includes a light streak running longitudinally along the vessel centre known as Central Vessel Reflex (CVR). It is more prominent in arteries than in veins because this phenomenon occurs at longer wavelengths that are more responsive to the blood oxygen content [27]. It is more visible in younger individuals than in adults [28]. This vessel reflex must be removed because the pixels intensities in the middle of the vessel are

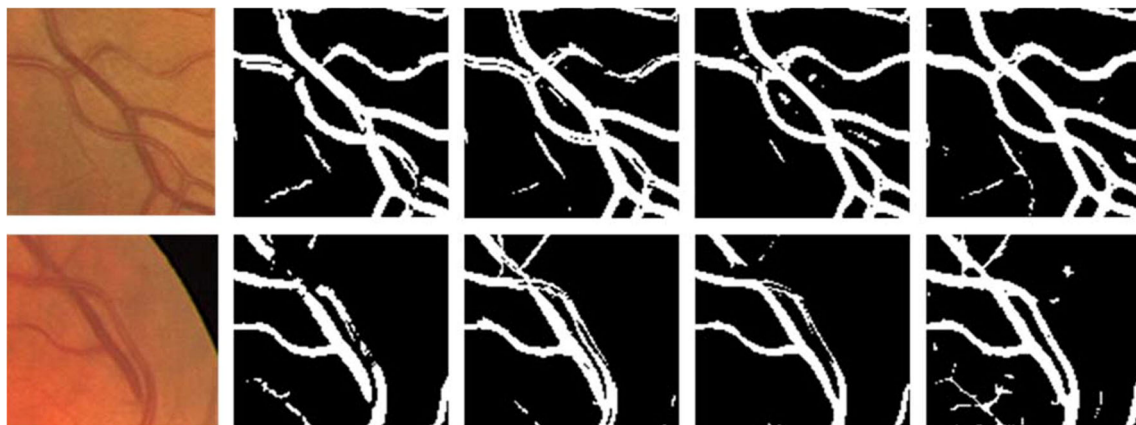


Fig. 5 Segmentation results on ROI showing the performance of various existing methods in the presence of CVR, close parallel vessels and bifurcation/crossover regions. First column: original image; second column: segmentations of Staal et al. [104] method; third

column: Soares et al. [39] method; fourth column: Ricci et al. [29] method; and fifth column: Nguyen et al. [24] method. (Illustrations based on material from Nguyen et al. [24], with kind permission from Elsevier)

Table 1 Summary of the vessel segmentation approaches presented in 56 papers considered in this study

	Authors	Method	Dataset		
Supervised	Fraz et al. [22]	GOA + MT + LSM + GFR + DT	DRIVE, STARE, CHASE.DB1		
	Condurache et al. [46]	HBC	DRIVE, STARE		
	Fraz et al. [28]	DG + SDG + GFR + LSM + MT + DT	CHASE.DB1		
	Welikala et al. [16]	MLO + SVM	MESSIDOR		
	Rahebi et al. [47]	GLCM + NN	DRIVE, STARE		
	Fathi et al. [48]	LBP + NN	DRIVE, STARE		
	Ganjee et al. [49]	MSMF + SRF	STARE		
	Orlando et al. [50]	CRF + SOSVM	DRIVE, STARE, CHASE.DB1, HRF		
	Wang et al. [54]	CNN + RF	DRIVE, STARE		
	Vega et al. [41]	LNNDP	DRIVE, STARE		
	Dai et al. [52]	GV + GW + GMM	DRIVE, STARE		
	Roychowdhury et al. [53]	FSOF + GMM	DRIVE, STARE, CHASE.DB1		
	Zhang et al. [71]	MTD + NN	DRIVE		
	Li et al. [55]	DAE	DRIVE, STARE, CHASE.DB1		
	Liskowski et al. [56]	DCNN	DRIVE, STARE, CHASE.DB1		
	Maninis et al. [57]	DCNN	DRIVE, STARE		
	Wu et al. [58]	DCNN + PF + NNS	DRIVE		
	Fu et al. [59]	CNN + CRF	DRIVE, STARE		
	Strisciuglio et al. [60]	B-COSFIRE + SVM	DRIVE, STARE		
	Unsupervised	Matched filtering	Abbasi et al. [101]	BIMSO	DRIVE, IOSTAR
Wang et al. [44]			MFMK + AT	DRIVE, STARE	
Krause et al. [61]			LRT	DRIVE	
Azzopardi et al. [23]			B-COSFIRE	DRIVE, STARE, CHASE.DB1	
Kovacs et al. [62]			GGF + CR	DRIVE, STARE, HRF	
Kar et al. [63]			CT + MF + LoG	DRIVE, STARE, DIARETDB1	
Zhang et al. [64]			LAD-OS	DRIVE, STARE, CHASE.DB1, HRF, IOSTAR, RC-SLO	
Multi-scale approach			Yu et al. [65]	HM + LET	DRIVE, STARE, HRF
			Moghimirad et al. [66]	MEF + HM	DRIVE, STARE
			Budai et al. [68]	HM + HT	DRIVE, STARE
		Nguyen et al. [24]	MSLD	DRIVE, STARE, REVIEW	
		Fathi et al. [38]	CCWT + AT + LF	DRIVE, STARE	
		Zheng et al. [67]	HM + NMF	DRIVE	
		Annunziata et al. [69]	NEBF + HM + PT	STARE, HRF	
		Abdallah et al. [70]	ADF + HM	DRIVE, STARE	
		Yin et al. [72]	OAD + GW + POF	DRIVE, STARE	
		Christodoulidis et al. [73]	MSLD + TVF	HRF	
Vessel tracking		Yin et al. [74]	MAP	REVIEW	
		Yin et al. [75]	MAP	DRIVE, STARE, REVIEW	
		Zhang et al. [76]	MAP + MSLD	REVIEW	
	De et al. [77]	TI	DRIVE		
	Bekkers et al. [78]	OS	HRF, REVIEW		
Mathematical morphology	Fraz et al. [43]	FDOG + MTHT + BPS	DRIVE, STARE, MESSIDOR		
	Fraz et al. [79]	FDOG + MTHT + RG	DRIVE, STARE		
	Sigurosson et al. [31]	POF + FC	DRIVE		
	Imani et al. [80]	MCA	DRIVE, STARE		

Table 1 (continued)

	Authors	Method	Dataset
Thresholding based approach	Roychowdhury et al. [42]	AGT	DRIVE, STARE, CHASE_DB1
	Mapayi et al. [81]	AT + GLCM	DRIVE, STARE
	Mapayi et al. [82]	AGT + CLAHE + PC	DRIVE, STARE
Model based approach	Xiao et al. [83]	BMSC	DRIVE, STARE
	Gonzalez et al. [84]	GC	DRIVE, STARE, DIARETDB1
	Zhao et al. [25]	ADF + LS + RG	DRIVE, STARE
	Zhao et al. [6]	RIC + LP + GC	DRIVE, STARE, ARIA, VAMPIRE
	Zhao et al. [40]	LP + IPAC	DRIVE, STARE, VAMPIRE
Other general approach	Hassanien et al. [86]	BSO + FCM + PSO	DRIVE, STARE
	Frucci et al. [87]	DM	DRIVE
	Lazar et al. [85]	MSMF + BHT + DRVM + RG	DRIVE, STARE, HRF

The approaches are mainly classified into supervised and unsupervised methods. The acronyms for the algorithms stand for: gradient orientation analysis (GOA), morphological transformation (MT), line strength measure (LSM), Gabor filter response (GFR), Decision trees (DT), Hysteresis binary classifier (HBC), Modified line operator (MLO), support vector machines (SVM), gray level co-occurrence matrix (GLCM), neural network (NN), local binary pattern (LBP), dual Gaussian (DG), second derivative of Gaussian (SDG), multi-scale matched filtering (MSMF), shape and region features (SRF), conditional random field (CRF), structured output support vector machine (SOSVM), gray voting (GV), Gabor wavelet (GW), Gaussian mixture model (GMM), first and second order features (FSOF), multiscale texton dictionary (MTD), convolutional neural networks (CNN), random forest (RF), lattice neural network with dendritic processing (LNNDP), deep autoencoders (DAE), deep convolutional neural network (DCNN), particle filtering (PF), nearest neighbor search (NNS), Bar - Combination of Shifted Filter Responses (B-COSFIRE), matched filtering with multi-wavelet kernels (MFMK), adaptive thresholding (AT), local radon transform (LRT), generalized Gabor function (GGF), contour reconstruction (CR), curvelet transform (CT), matched filtering (MF), Laplacian of Gaussian filter (LoG), locally adaptive derivative on orientation score (LAD-OS), hessian matrix (HM), local entropy thresholding (LET), medialness function (MEF), non-local means filtering (NMF), multiscale line detection (MSLD), complex continuous wavelet transform (CCWT), length filtering (LF), hysteresis thresholding (HT), percentile thresholding (PT), neighbourhood estimator before filling (NEBF), anisotropic diffusion filtering (ADF), orientation aware detector (OAD), path opening filter (POF), tensor voting framework (TVF), maximum a posteriori estimation (MAP), transductive inference (TI), orientation scores (OS), first order derivative of Gaussian (FDOG), morphological top-hat transform (MTHO), bit plane slicing (BPS), region growing (RG), fuzzy classification (FC), morphological component analysis (MCA), morlet wavelet transform (MWT), adaptive global thresholding (AGT), phase congruency (PC), contrast limited adaptive histogram equalization (CLAHE), Bayesian model with spatial constraint (BMSC), graph cut (GC), level sets (LS), retinex-based inhomogeneity correction (RIC), local phase-based enhancement (LP), infinite perimeter active contour (IPAC), directional response vector map (DRVM), bottom-hat transform (BHT), bee colony swarm optimization (BSO), fuzzy c-means (FCM), pattern search optimization (PSO), direction map (DM), brain inspired multi-scales and multi-orientations (BIMSO)

much lower than its surroundings leading to false detection of two close vessels instead of a single vessel.

The classical technique for removal of CVR is morphological opening. In this method, the morphological opening is performed using three-pixel diameter disc, defined on a square grid by using eight-connectivity as a structuring element. Ricci et al. [29] initially proposed a basic line detector for vessel segmentation which deals with vessel reflex in an efficient way. This method is based on the average grey level response of a fixed line length passing through the target pixel at different orientations. The limitation of the basic line detector is that it tends to merge close parallel vessels and produces false detections near bifurcation/crossover regions (see Fig. 5). To overcome this limitation, Nguyen et al. [24] proposed a method based on the response of basic line detector on various scales and varying the length of the line. This multi-scale line detector can recognize vessel reflex as a part of a vessel since the average line response is not affected much because the central reflex constitutes only small number of pixels compared to its surrounding vessel pixels (see Fig. 5).

Intensity inhomogeneity correction

During image acquisition, retinal fundus images often contain background intensity variation caused by non-uniform illumination. This influences the performance of the vessel segmentation algorithms. Among the several methods proposed in the literature, histogram equalization is commonly employed for intensity inhomogeneity correction. The drawback of this approach is that it cannot handle color images and pixels intensities spanning the whole range of display devices. Another popular enhancement technique is gamma correction, which enhances images that are either too dark or too bright. But this method is image dependent. A well known technique for luminosity and contrast normalization in retinal images was proposed by Foracchia et al. [105]. In this method, the Luminosity and contrast variability in the background part of the image is estimated and then used for the normalization of the whole image. Normalization is performed on both intra and inter images.

One of the most promising method used in the literature is Contrast-Limited Adaptive Histogram Equalization (CLAHE) technique proposed in [95]. In this approach, the image is divided into contextual regions that are then individually enhanced using histogram equalization. The clipping level of the histogram is chosen by computing the local histogram mapping function. This can reduce the amplification of noise in similar regions. Azzopardi et al. [30], Welikala et al. [16], Sigursson et al. [31], Zhao et al. [25] have adopted this technique. But the problem with this method is that if there is a bright or dark lesion next to the vessel, the lesion location is further enhanced leading to difficulty in distinguishing between vessel and lesion structure.

Fraz et al. [32] proposed a method, based on subtracting an estimate of the image background (which is obtained by applying an arithmetic mean kernel by using decimation) from the original image. The most recent and effective technique for intensity inhomogeneity correction was proposed by Zhao et al. [6] and is based on Retinex theory (see Fig. 6). In [6], an image is modelled as a multiplication of two components, the reflectance and the illumination. The reflectance component of the image reveals the object of interest more clearly, and it can be considered as the enhanced version of an image.

Vessel enhancement

The retinal image constitutes varying anatomical structures in their size, complex shapes and orientation such as blood vessels, optical disc, and background tissues. The problem with vessel segmentation is, the complexity of vascular structures near the thin vessels and bifurcation/crossover regions. So, it is often necessary to enhance

vessel structures. Chaudhuri et al. [33] were the first to investigate the vessel enhancement technique by applying matched filters. It is based on Gaussian shape modelling of vessel cross-sectional profile of the retina. But the major drawback of this approach is, it cannot effectively enhance vessels of varying width at a single scale. On the other hand, even by adopting multiple filters with various scales, some fine vessels cannot be detected due to the low-density contrast and relatively heavy background noise.

Most of the retinal vessel enhancement filters found in the literature are based on image intensity profile. Some of the prominent intensity based filters are matched filters [33], amplitude-modified second order Gaussian filter [34], Eigenvalue based filter [35], multi-scale linear operators [36], wavelet [37], [38], Gabor filter [39] and COSFIRE filter [23, 30]. But the drawback with the aforementioned intensity based filters is, they are more prone to non-uniform illumination present in the image. In contrast, filters based on local phase information [6, 40] of an image is an emerging technique which can avoid the problems faced by the intensity based filters. Local Phase (LP) filters can be estimated by quadrature filters under the concept of monogenic signals for two or higher dimensions. These LP filters can show consistent results at the bifurcation and crossover regions when compared to the other parts of the vessels (see Fig. 7). Thus, indeed it can be applied to solve the complex segmentation problem at vessel crossings and bifurcations regions.

Another well-known vessel enhancement technique reported in the literature is the use of morphological filters such as top hat transform [22, 28, 31, 41–43]. These morphological filters can enhance the image regions by estimating local background by a morphological opening operation, which is then subtracted from the original image.

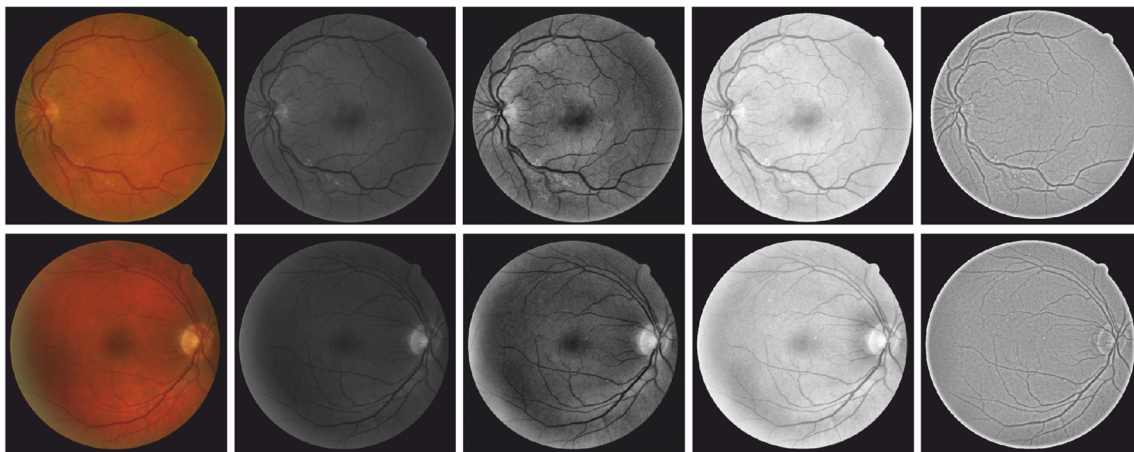


Fig. 6 A comparative study on image-wise enhancement techniques. First column: two example images from the DRIVE dataset; second column: the green channel image; third and fourth column: results after applying Histogram Equalization and Gamma correction image

enhancement methods; fifth column: results after applying Retinex. (Illustrations based on material from Zhao et al [6], with kind permission from PloS one)

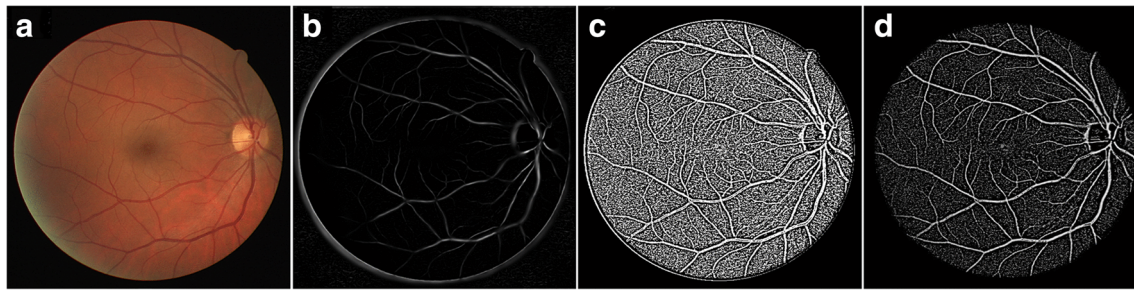


Fig. 7 Vessel enhancement results using different methods. **a** A randomly chosen image from the DRIVE dataset, **b** Eigenvalue-based [35], **c** wavelet-based [37], and **d** Local Phase-based [6] enhancements

One of the recent technique reported in the literature is matched filters with multi-wavelet kernels (MFMK) proposed by Wang et al. [44]. These MFMK methods can separate vessels from clutter edges and bright localized areas such as lesions. Finally, the effects of each pre-processing step might affect each segmentation technique differently making any implicit generalization difficult. The comparison of the above preprocessing steps and their interaction with segmentation performance is quite complex and beyond the scope of this paper.

Segmentation methods

In this section, we review the most recent techniques proposed for retinal vessel segmentation in the last five years. Table 1. summarizes the vessel segmentation methods presented in 56 papers published between 2012 and 2016 along with the datasets used for performance evaluation. In this review, we mainly focus on methods applied to color fundus images, FA and SLO images, since most of the earlier methods have been evaluated on these three modalities.

Broadly, all the previously published segmentation methods can be divided into two main categories, supervised and unsupervised. Supervised methods require a manually annotated set of training images for classifying a pixel either as a vessel or a non-vessel in previously unseen images. In these methods, typically we extract features for each pixel along with their true label to learn a model of a classifier. Most of the techniques in this category are k-nearest neighbors, Support Vector Machine (SVM), Neural Networks (NN), Gaussian Mixture Models (GMM), AdaBoost, Conditional Random Fields (CRF) and the recent Convolutional Neural Networks (CNN) etc. On the contrary, unsupervised methods can segment the vessels without requiring any labelled annotations. In general, most of these techniques are based on the response of matched filters, morphological processing, vessel tracing, thresholding, region growing, multi-scale approaches, etc. In the following section, we

briefly explain the essence of these techniques and discuss how these methods perform segmentation of vessels in challenging conditions, followed by strength and weakness of these methods.

Supervised methods

Supervised methods are based on pixel classification where the primary objective is to segment retinal vessels by training a set of manually annotated gold standard images. Often these gold standard images are annotated by experienced ophthalmologists. The most discriminative set of feature vectors must be selected from the set of training images for better classification of the vessel and non-vessel structures. In general, the performance of supervised methods is better than that of unsupervised ones.

Fraz et al. [22], [28] proposed a novel method in this category based on combination of multiple feature extraction techniques such as orientation analysis of gradient vector field, morphological transformation, line strength measure, and Gabor filter response. Classification of pixels were performed using an ensemble of weak learners such as decision trees. Most of the earlier techniques were evaluated on DRIVE and STARE dataset which consists of fewer number of images. In contrast, Fraz et al. [22] created a new database known as CHASE_DB1 which was primarily used to study the cardiovascular risk factors in younger individuals. The addition of CHASE_DB1 provides an opportunity for the researchers to evaluate their method on this challenging dataset due to the presence of CVR and illumination artefacts.

Condurache et al. [46], adopted a binary classification technique based on hysteresis classification paradigm. Their method is well suited for binary classification problem afflicted by significant class skew and overlap between classes such as vessels and background structures. Welikala et al. [16], proposed a dual classification approach for the segmentation of new blood vessels. The algorithm is more reliable for automated detection of PDR where there is a

high-risk progression of new blood vessels (see Fig. 3b). A method based on gray level co-occurrence matrix (GLCM) and neural network (NN) classifier was proposed in [47]. A novel segmentation technique based on non-linear invertible orientation scores is presented in Abbasi et al. [101]. According to authors, the method [101] is robust against noise, non-uniform illumination and contrast variability. In addition to preserving the vessel connectivity, it has higher sensitivity and detects the small vessels better than the state-of-the-art methods for both RGB and SLO images.

An effective technique to deal with pathological images was proposed in [49]. Their method adopted a combination of multi-scale matched filtering along with shape and region-based features to distinguish between vessel and lesion structures. A combination of first and second order gradient features along with Gaussian Mixture Model (GMM) classifier was used in [53]. Strisciuglio et al. [60] proposed an efficient method for segmenting vessels in pathological images using a selective set of B-COSFIRE filters by means of different feature selection methods. For the first time in the literature, conditional random fields for retinal vessel segmentation have been proposed by Orlando et al. [50]. In their method, a fully connected CRF is trained using structured output SVM in a supervised manner. Their approach was able to solve the poor segmentation problem due to weak priors assigned to an elongated structure as in the case of standard pairwise potential.

Recently, Cheung et al. [51] observed that the micro-vascular structures (thin vessels) in the retina play a vital role in the early diagnosis of diseases such as stroke, Alzheimer's and other micro-vascular diseases. In contrast, segmentation of thin vessel structures in the retina is extremely difficult compared to the large vessels. To overcome this limitation, Dai et al. [52] proposed a gray voting technique based on local gray level statistics. Their method enhances small vessel structures and has shown promising results. Further, a general extension of Local Binary Pattern (LBP) operator was proposed in [48] with NN classifier to segment the thin vessels. Zhang et al. [71] adopted a multiscale texon dictionary and NN classifier to classify vessel/non-vessel pixels. A Gabor filter bank is used to extract features which are then used as initial key points to initialize k-means clustering which builds a texon dictionary ultimately.

Inspired by the success of deep learning techniques in computer vision applications, Convolutional Neural Network (CNN) has emerged as a promising approach to solve segmentation problems in medical imaging applications. In this context, Wang et al. [54], proposed a segmentation method by employing CNN and ensemble of random forests. Later, Vega et al. [41] adopted a new generation of neural network known as Lattice Neural Network (LNN). Some of the interesting properties of LNN are, there are

no convergence problems with a single layer feed forward neural network and does not involve any hidden layers. Li et al. [55], proposed a cross-modality approach using deep autoencoders. A deep neural network is used to model the relationship between the retinal image and the vessel map. The proposed approach works well in the presence of CVR, pathological images, and thin vessel structures.

The most recent approach by Liskowski et al. [56] proposed a deep neural network model. Their method was able to achieve an area under the curve (AUC) of 0.99, which is significantly better than all previously published methods in the literature. The method is also robust to CVR and performs reasonably well on pathological images. A novel CNN architecture was proposed in [57] to solve both the retinal vessel and optic disc segmentation problem. Wu et al. [58] proposed a DCNN architecture under a probabilistic tracking framework, designed with generalized particle filtering technique to extract retinal vessel tree. Later, Fu et al. [59] formulated the vessel segmentation as a boundary detection problem using fully connected CNN model. A fully connected CRF's is utilized further to take into account the long-range interaction between the pixels.

Unsupervised methods

The unsupervised segmentation methods work without prior knowledge and labelled groundtruths. In general, most of these methods are rule-based techniques which include conventional matched filtering, morphological processing, vessel tracing, thresholding, region growing, multi-scale approaches, etc. The unsupervised methods generally have a higher speed and lesser computational complexity compared to supervised ones.

Matched filtering

Matched filtering (MF) involves convolving an image with a 2-D Gaussian template. These methods exploit the fact that the vessel cross-sectional intensity profile can be modelled as a Gaussian shaped curve. But these assumptions often fail in the presence of CVR. Hence several variants of the MF have been proposed in the literature to overcome this limitation. The earliest approach of using 2-D matched filters for vessel segmentation was proposed in Chaudhuri et al. [33]. Later, Wang et al. [44], extended the idea of matched filtering in combination with multi-wavelet kernels to separate the blood vessels from lesion structures. To enable the faster and parallel implementation, Krause et al. [61] employed local Radon transform for retinal vessel segmentation. They have segmented 20,000 images of size $2,048 \times 1,536$ in about 3 hours on a NVIDIA Geforce GTX680. This is one of the most recent methods in implementing the segmentation algorithm on the GPU-based platform with a very low

time complexity. Another well known method in this category is based on B-COSFIRE (Bar - Combination of Shifted Filter Responses) filter proposed by Azzopardi et al. [23]. The idea behind their approach is that COSFIRE filter can selectively respond to bar-shaped (linear) structures such as vessels.

Kovacs et al. [62] proposed a self-calibration technique which can be used to transform a trained model to retinal images of different resolution, field-of-view (FOV), noise level, etc. The segmentation method was based on template matching using Gabor filters and contour reconstruction strategies. Kar et al. [63] proposed a combined approach using curvelet transform, matched filtering and Laplacian of Gaussian filter. Their experimental results in [63] shows that the method performed well on both pathological as well as noisy retinal images. Zhang et al. [64] proposed a segmentation technique based on maximizing the multi-scale second-order Gaussian derivatives filter response in the orientation score domain. The method has been evaluated on six publicly available databases including the SLO images such as IOSTAR and RC-SLO datasets. Their approach has shown better segmentation performance at vessel crossings, CVR, closely parallel and tiny vessels.

Multi-scale approach

Retinal vessel structures appear at multiple scales and orientation in an image. This property has been exploited in the literature to capture vessel structures of varying width and direction. The advantage of these methods is both major and minor vessels can be segmented effectively. Among the techniques proposed in this category, the earliest approach by Yu et al. [65] is based on Eigen analysis of the Hessian matrix followed by second-order local entropy thresholding. Their method had a few drawbacks: first, it tends to over segment the major vessels including pathological lesions; second, it under-segments the thin vessels. To overcome these limitations, Moghimrad et al. [66] proposed a method based on multi-scale medialness function initially intended for tubular structure extraction. Most of the tubular structure extraction schemes are based on Eigen analysis of the Hessian matrix. But the problem with these methods is that the response of the Eigenvalues of the Hessian matrix is weaker in the area of bifurcation/crossover points. To address these issues, authors in [66] proposed a combined approach of Hessian matrix and 2-D medialness function. The advantage of their method is that it provides better segmentation at bifurcation and crossover regions. Zheng et al. [67] proposed multi-scale Hessian matrix based non-local filtering approach to enhance the vessel structures and suppress the background noise.

Nguyen et al. [24] introduced the concept of multiscale line detection (MSLD) for vessel segmentation. This idea

was the initial extension of basic line detection method proposed by Ricci et al. [29]. In comparison to [29], their method overcomes the limitation of poor segmentation near two closely parallel vessels and at crossover points. Later, Yin et al. [72] modified the idea proposed in [24] to design a novel orientation aware detector to segment both major and minor vessels. Their method works well in the presence of CVR, close vessels, and crossover points. The main limitation of the line detector methods is that it is unable to segment smallest vessels. This drawback has been addressed by Christodoulidis et al. [73] by adopting a hybrid approach based by combining MSLD and multi-scale tensor voting procedure. This approach has shown a better segmentation performance on thin vessel structures compared to other previous methods.

Fathi et al. [38] proposed a complex continuous wavelet transform (CCWT) with an adaptive histogram based thresholding method for segmentation of vessels. Vessel diameter estimation has also been addressed by employing circular structure descriptor on the centerline of the vessels. Budai et al. [68] proposed an improvement over the vessel enhancement method initially proposed in [35]. A novel approach based on inpainting technique was suggested by Annunziata et al. [69] to inpaint the false vessel structures (such as exudates) in pathological images. Their method significantly reduces the number of false positives in pathological images. A multiscale line tracking procedure was proposed in [70] based on the fact that the vessel structures appear at multiple scales and orientation in an image.

Vessel tracing

In vessel tracing methods, initial seed points are chosen either manually or automatically both on the edges and centerline of the vessels. Given these initial seed points, the entire vessel tree is traced by following vessel centerline based on local information. Since the vessels are connected in the retina, tracing methods can follow a whole tree structure without explicitly monitoring the background. These methods provide a precise vessel connectivity information at branching and crossovers points for early detection of many systemic diseases.

The method in this category was proposed in Yin et al. [74, 75] based on maximum a posteriori (MAP) formulation. The initial vessel edge points are detected iteratively using local grey level statistics and vessel continuity properties. A Gaussian-shaped curve is fitted to the intensity profile of local vessel cross-section to estimate the vessel appearance. Similar to the previous work, Zhang et al. [76] proposed a combined approach using MAP criterion and multiscale line detection method. In their work, the authors succeed in differentiating between normal, branching and crossover vessels. A principled way of addressing

the crossover issue has been solved in De et al [77] based on transductive learning approach. Their method performs better in resolving many complex bifurcation/crossover points. Inspired by the modelling of cortical columns in the primary visual cortex, Bekkers et al. [78] proposed a multi-orientation vessel connectivity analysis near bifurcation and crossing regions. Among all the tracing methods, their approach was able to successfully track and measure width even at complex locations.

Mathematical morphology

Mathematical morphology is a powerful tool based on set theory concept, mainly used for extracting complex image structures that provide useful representation and description of region shapes such as features, boundaries, skeletons and convex hulls. These methods exploit the fact that the vessels are linear and connected in the retina. These methods are also known for its speed and noise resistance. The main drawback of these methods is, they fail to model the highly curved vessels which are more prominent in younger individuals.

Among the methods in this category, Fraz et al. [43, 79] proposed a novel approach for identifying both vessel centerline and segmentation of vascular tree. The vessel centerlines are identified using the first order derivative of a Gaussian filter followed by a multi directional morphological top-hat transform to segment the vessels. The main limitations in [43, 79] is difficulty in modelling the highly curved and tortuous vessels. Later Sigursson et al. [31] addressed this challenge by proposing a novel approach based on path opening filter followed by a fuzzy set theory based data fusion technique. Their method demonstrated an ability to distinguish between major and minor vessels with a better accuracy than the other methods. The traditional problem of vessel segmentation in the presence of abnormalities was tackled in Imani et al. [80]. In their method, morphological component analysis (MCA) combined with Morlet Wavelet Transform (MWT) was used to separate vessels from other lesion structures which are crucial in clinical settings for the assessment of abnormal cases.

Thresholding based approach

Among the most recent thresholding based approaches, Roychowdhury et al. [42] proposed a method which can efficiently handle vessel segmentation in the presence of abnormalities as well as thin vessel structures. Their method adopted an iterative vessel segmentation approach by employing global adaptive thresholding followed by a novel stopping criteria. Further, Mapayi et al. [81] proposed a local adaptive thresholding technique based on GLCM energy information for segmenting retinal vessels. Their method provides

robust segmentation for both grayscale and green channel intensity of RGB retinal images. Later, Mapayi et al. [82] proposed a approach based on global thresholding with phase congruency and CLAHE for segmentation of vessels.

Model based approach

Model based approaches consist of vessel profile models and deformable models. In vessel profile models, the vessel cross-sectional intensity profile is modelled as a Gaussian-shaped curve or mixture of Gaussians in the case of CVR. In deformable models, both active contour and level set based approaches are employed. Among the methods in this category, Xiao et al. [83] presented a Bayesian based segmentation approach which takes into account the spatial information. Their method results in better performance in the detection of both narrow and low contrast vessels. Further, Gonzalez et al. [84] presented a combined framework for both vessel and optic disc segmentation problem. Their method adopted a graph cut technique to segment the vessel tree followed by MRF image reconstruction and compensation factor method to segment the optic disk. Zhao et al. [25], adopted two separate techniques for extracting both major and minor vessels from retinal images. For major vessels, a level set method based on region-scalable fitting energy function is applied, and for minor vessels, a region growing approach is adopted.

Recently, a novel inhomogeneity correction method based on Retinex theory and LP analysis was proposed in Zhao et al. [6] for vessel enhancement. In their work, the authors have shown the comparative analysis of various existing preprocessing methods in the literature along with their proposed one (see Figs. 6 and 7). Adopting the similar preprocessing technique proposed in [6], Zhao et al. [40] proposed a segmentation approach based on infinite perimeter active contour model utilizing hybrid region information of the image. For the first time in the literature, the authors in [40] have evaluated their segmentation technique on FA images which could open further research directions in retinal image analysis.

Other general approach

The methods published in this category include those that belong to general image processing based techniques that are adapted for segmenting retinal vessels. Hassanien et al. [86] proposed the idea of two-level optimization for segmenting thin vessel structures. The first level includes finding the vessel clusters with artificial bee colony swarm optimization using fuzzy c-means fitness function. In the second level, pattern search algorithm is enhanced by adding shape descriptors as an additional feature in the fitness function. Later, Frucci et al. [87] used the concept of directional map

for segmenting vessel structures. The advantage of their method is, it is computationally less intensive and requires no preprocessing steps. Finally, Lazar et al. [85] proposed a hybrid region growing approach based on directional response vector similarity of pixels along with a nearest neighbor classifier.

Summary of vessel segmentation methods

Among the recent methods published in the literature, supervised methods based on deep learning architecture [55, 56] has surpassed all other techniques in obtaining the performance very close to (or even outperforming) trained human observers. These methods are able to successfully address most of the challenges posed by the complex nature of vessel structures as discussed in “Challenges in retinal vessel segmentation”. The success of these methods is mainly due to larger computational power and the addition of large datasets. The main advantage of CNN based methods is that they don’t require any carefully hand-crafted features and complex domain expertise. In contrast, these methods are able to successfully learn the complex nature of vessel structures even in the most challenging cases (like the presence of thin vessel structures and abnormalities). A new wave of CNN methods have been recently proposed in the literature such as [58, 59] manifesting a special interest in the community towards the development of newer deep learning based architectures for retinal vessel segmentation.

Table 2 depicts the segmentation challenges addressed by recent state-of-the-art methods. The newer methods like [25, 31, 42, 48, 52, 62, 73, 83] has explicitly proposed techniques for segmentation of thin vessel structures. Christodoulidis et al. [73] proposed a combined approach of MSLD along with multiscale tensor voting for detection of major and minor vessel structures. This is one of the first kind in segmentation methods that has specifically considered the segmentation of thin vessels and has shown remarkable performance. The problem of CVR, poor segmentation near bifurcation/crossover points and close parallel vessels have been addressed in Nguyen et al. [24]. Other methods like Zhao et al. [6, 40] has considered the problem of intensity inhomogeneity and vessel enhancement techniques on low contrast images. Although the most recent methods have shown interest in addressing the segmentation challenges, there is a still room for future improvements towards the building of successful retinal CAD systems.

Review of validation

In this section, we analyze the quantitative assessment of segmentation methods proposed in the current state-of-the-

Table 2 Segmentation challenges addressed by recent state-of-the-art methods

Authors	PL	TV	CVR	BC	IN
Fraz et al. [22]	Yes	—	Yes	—	—
Fathi et al. [48]	—	Yes	—	—	—
Fraz et al. [28]	—	—	Yes	—	—
Ganjee et al. [49]	Yes	—	—	—	—
Orlando et al. [50]	—	—	—	—	Yes
Dai et al. [52]	—	Yes	—	—	—
Roychowdhury et al. [53]	Yes	—	—	—	—
Li et al. [55]	Yes	Yes	Yes	Yes	Yes
Liskowski et al. [56]	Yes	Yes	Yes	Yes	Yes
Fu et al. [59]	Yes	—	—	—	—
Zhang et al. [64]	Yes	Yes	Yes	Yes	Yes
Strisciuglio et al. [60]	Yes	—	—	—	—
Wang et al. [44]	Yes	—	—	—	—
Azzopardi et al. [23]	—	—	—	Yes	—
Kovacs et al. [62]	—	Yes	—	—	—
Kar et al. [63]	Yes	—	—	—	Yes
Moghimirad et al. [66]	—	—	—	Yes	—
Zheng et al. [67]	—	—	—	—	Yes
Nguyen et al. [24]	—	—	Yes	Yes	—
Annunziata et al. [69]	Yes	—	—	—	—
Yin et al. [72]	Yes	—	Yes	Yes	—
Christodoulidis et al. [73]	Yes	Yes	—	—	—
Yin et al. [74]	—	—	—	Yes	—
Zhang et al. [76]	—	—	Yes	Yes	—
De et al. [77]	—	—	—	Yes	—
Bekkers et al. [78]	—	—	—	Yes	—
Sigurosson et al. [31]	—	Yes	—	—	—
Imani et al. [80]	Yes	—	—	—	—
Roychowdhury et al. [42]	Yes	Yes	—	—	—
Xiao et al. [83]	—	Yes	—	—	—
Zhao et al. [25]	—	Yes	—	—	—
Zhao et al. [6]	—	—	—	Yes	Yes
Zhao et al. [40]	—	—	—	—	Yes

The acronyms stand for: robust to pathological lesions (PL), able to segment thin vessel structures (TV), robust to central vessel reflex (CVR), better segmentation near bifurcation/crossover regions (BC), robust to intensity inhomogeneity, blur and noise present in the image (IN)

art, including the datasets employed and measures performed. Some significant findings of the existing techniques and few open problems are also been discussed.

Retinal image databases

Retinal image segmentation methods in the literature are evaluated using different quantitative measures and different

publicly available datasets. Most of the existing state-of-the-art methods have been evaluated on publicly available: DRIVE [88], STARE [89], CHASE_DB1 [22] and HRF [91] databases. Few methods have also made an attempt to validate their technique on other databases like ARIA [90], DIARETDB1 [92], MESSIDOR [93], REVIEW [94], VAMPIRE [96], IOSTAR [97] and RC-SLO [98]. An overview of the aforementioned publicly available datasets is provided in Table 3.

The earliest datasets like DRIVE and STARE includes fewer number of images ranging from 20 to 40. All of these images mainly consists of healthy images and fewer pathological cases. With the recent advancements in newer high-resolution fundus camera, it is now possible to obtain much higher resolution 3504×2336 images as in HRF dataset when compared to lower resolution 768×584 images in case of DRIVE. As discussed in “Challenges in retinal vessel segmentation”, there is a requisite for thorough evaluation of segmentation methods particularly on abnormal

cases which is required for clinical scenarios. Such images can be found in STARE, ARIA and HRF datasets which contain cases of DR, AMD, and Glaucoma. Recently, Fraz et al. [22], introduced a new database CHAS-E_DB1 which includes images of multi-ethnic school children which was primarily used for quantification of changes in retinal vessel width in relation to cardiovascular disease in later life. Recently, Zhang et al. [64] published two newer datasets: IOSTAR [97] and RC-SLO [98] based on the SLO technique. These two datasets cover a wide range of challenging cases, such as high curvature changes, CVR, micro-vessels, crossings/bifurcations.

Validation measures

Four primary validation measures have been commonly employed to evaluate the performance of vessel segmentation methods. They are Se (Sensitivity), Sp (Specificity), Acc (Accuracy) and AUC (Area under the curve). Several

Table 3 Overview of publicly available retinal image datasets

Dataset	Year	Description	Image size and FOV	Vessel groundtruth (Reference standard)
STARE [89]	2000	Total 20 color fundus images. out of which 10 are healthy and 10 are pathological.	700×605 35°	Groundtruths are annotated by two human observers.
DRIVE [88]	2004	Contains 40 color fundus images. It is divided into 20 for training and 20 for testing.	584×565 45°	Groundtruths are annotated by two human observers.
MESSIDOR [93]	2004	Contains 1200 color fundus images. Contains pathological signs such as microaneurysms, hemorrhages, neovascularization and hard exudates.	1440×960 , 2240×1488 , 2304×1536 45°	No vessels groundtruth are available. Reference standard is available for grading of diabetic retinopathy and the risk of macular edema.
ARIA [90]	2006	Total of 212 color fundus images: first group: 92 AMD images second group: 59 DR images third group: 61 normal images	768×576 50°	The reference standard for optic disc, blood vessel tracking and fovea location is marked by two clinical experts.
DIARETDB1 [92]	2007	Consists of 89 retinal images. Out of which 84 contain signs of DR and 5 are normal.	1500×1152 50°	Manually segmented retinal vasculature is not available for this database.
REVIEW [94]	2008	Contains 16 images with 193 annotated vessel segments consisting of 5066 profile points	—	Vessel widths are manually marked by three independent experts.
CHASE_DB1 [22]	2011	Contains 28 color fundus images. Out of which 20 corresponds to testing and 8 for training.	1280×960 30°	Vessel segments and width are annotated by two clinical experts.
HRF [91]	2011	Contains 45 color fundus images: first set: 15 healthy images second set: 15 DR images third set: 15 glaucoma images	3304×2336 60°	Reference standard was provided by three clinical experts.
VAMPIRE [96]	2011	8 retinal FA images. Out of which 4 contains AMD.	3900×3072 200°	Groundtruth was provided by three clinical experts.
IOSTAR [97]	2015	Includes 30 SLO images	1024×1024 45°	Vessels are annotated by a group of experts
RC-SLO [98]	2015	Contains 40 SLO image patches	360×320 —	Vessels are annotated by a group of experts

newer validation measures for vessel segmentation have also been reported in the literature which is provided in Table 4.

Since retinal vessel segmentation is a binary classification problem, the commonly accepted measures include: True positive (*TP*) - Number of correctly classified vessel pixels, False negative (*FN*) - number of incorrectly classified vessel pixels, True negative (*TN*) - Number of correctly classified background pixels and False positive (*FP*) - Number of incorrectly classified background pixels. Based on these key measures, different performance parameters can be estimated such as *Se*, *Sp*, *Acc* and *AUC*. Sensitivity indicates the capability of the algorithm to correctly detect retinal vessels while specificity indicates the ability to distinguish all other non-vessel structures. Accuracy measures the ratio of correctly classified pixels (both vessel and non-vessel) to the total number of pixels in the image field of view. All these measures are obtained through the pixel to pixel comparison between automated segmentation and reference groundtruth. Most of these measures are suitable if the class data is balanced (equal number of positive and negative classes). But in the case of retinal images, the negative class samples (background pixels) outnumber the positive class samples (vessel pixels). By contrast, the presence of class imbalance in the data has a profound impact on these performance measures.

The aforementioned validation measures provide global information on segmentation quality without taking into account that the detected pixels are part of a vessel structure with specific features. Hence, more suitable validation measures for class imbalance data are included in Orlando et al. [50] and Azzopardi et al. [23] such as Matthews Correlation Coefficient (*MCC*), *F1 - score* and *G - mean*. The *MCC* is a correlation coefficient between the groundtruth and the predicted binary segmentation which returns a value between -1 and +1. With +1 indicating a perfect

prediction, 0 no better than random, and -1 a total disagreement between prediction and groundtruth. The *F1 - score* is the harmonic mean of precision and recall which achieves maximum value of 1 when the segmentation of the positive class is perfect, and lowest value of 0 when the segmentation is completely wrong. Similarly, the *G - mean* is a metric that measures the balance between *Se* and *Sp* by taking their geometric mean, returning a value between 0 and 1. The most common overlap metric, the Dice coefficient (*DC*) is also used for comparing the agreement between the manual annotations and the result of segmentation method. The *DC* ranges from 0 (no agreement) to 1 (perfect agreement).

Recently, Arias et al. [99], proposed a new measure called Quality Evaluation Function (*QEF*) based on the characterization of vascular structures as connected segments with the measurable area and length. This measure is sensitive to anatomical vascularity features. Hence, it is highly desirable in evaluating segmentation methods on pathological images. The *QEF* function has also shown a high degree of matching with human quality perception when compared to other measures reported in the literature.

Assessment of retinal vessel segmentation methods

The performance evaluation of segmentation methods significantly varies across the datasets. The main reasons for this are:

- Input images of different resolution across the data-sets as shown in Table 3.
- Different morphological attributes of the images like pathological lesions, varying tissue structures, intensity homogeneity and noise inherited due to various scanning protocols.
- Intra and inter-observer variability among the groundtruth annotations across and within the datasets.

Table 4 Overview of validation measures used for quantitative assessment of retinal vessel segmentation methods

Validation measure	Description
Sensitivity (<i>Se</i>)/Recall (<i>Re</i>)	$\frac{TP}{TP+FN}$
Specificity (<i>Sp</i>)	$\frac{TN}{TN+FP}$
Accuracy (<i>Acc</i>)	$\frac{TP+TN}{TP+TN+FP+FN}$
Area under curve (<i>AUC</i>)	$\frac{Se+Sp}{2}$
Precision (<i>Pr</i>)	$\frac{TP}{TP+FP}$
Matthews Correlation Coefficient (<i>MCC</i>)	$\frac{\frac{TP}{N} - S \times P}{\sqrt{P \times S \times 1 - S \times 1 - P}}$
F1 score (<i>F</i>)	$N = TP + TN + FP + FN, S = TP + FN \times N, P = TP + FP \times N$ $\frac{2 \times Pr \times Re}{Pr + Re}$
G - mean (<i>G</i>)	$\sqrt{Se \times Sp}$
Dice Coefficient (<i>DC</i>)	$\frac{2(A \cap B)}{A + B}$
Quality Evaluation Function (<i>QEF</i>)	$f(C, A, L) = C \times A \times L = CAL$

In this regard, we have considered the assessment of segmentation methods on an individual dataset for fair evaluation of previously published methods. We have considered four performance metrics for evaluation: *Se*, *Sp*, *Acc* and *AUC*. We have compared the segmentation techniques on four main datasets: DRIVE, STARE, CHASE_DB1 and HRF as depicted in Table 5. The values presented in the table are taken as it is reported in the corresponding articles.

Table 5 depicts the performance evaluation of different methods on DRIVE dataset. Among these methods, the highest reported *Se* of 0.9094 (Condurache et al. [46]), *Sp* of 0.9870 (Budai et al. [68]), *Acc* of 0.9767 (Wang et al. [54]) and *AUC* of 0.9790 (Liskowski et al. [56]). No single method was able to achieve the best results concerning all the metrics. When compared to all other datasets, vessel segmentation on DRIVE is relatively easy as most of the images are healthy with no pathological signs, vessels are clearly visible, and images are not much affected by illumination. One of the key observation is that most of the methods that reported the highest performance measures on DRIVE belong to the class of supervised methods.

Among the methods on STARE dataset, the highest reported *Se* of 0.9289 (Liskowski et al. [56]), *Sp* of 0.9844 (Li et al. [55]), *Acc* of 0.9813 (Wang et al. [54]) and *AUC* of 0.9930 (Liskowski et al. [56]). If we observe carefully, mostly supervised and multiscale methods have outperformed other methods in both DRIVE and STARE datasets. As discussed earlier in “Supervised methods” and “Multi-scale approach”, learning based methods (supervised) and multiscale methods (based on Hessian matrix), have shown remarkable performance. The success of these methods is because: (a) Due to inheriting multiscale nature of vessels which appears both thin and thick structures at various scales and orientation. (b) Learning the complex structures directly from the data as opposed to handcrafting those features based on domain expertise. The main drawback of the supervised methods is that, it requires pixel-level annotations for learning the correspondence during the training phase and much more computationally expensive than the other category of methods.

Among the published methods on CHASE_DB1 datasets, the highest reported *Se* of 0.8793 (Liskowski et al. [56]), *Sp* of 0.9793 (Li et al. [55]), *Acc* of 0.9581 (Li et al. [55]) and *AUC* of 0.9845 (Liskowski et al. [56]). This dataset is newly released compared to earlier DRIVE and STARE databases. The resolution of the images in CHASE_DB1 is of 1280×960 as opposed to 584×565 in DRIVE and 700×605 in STARE datasets. Another dataset which contains high-resolution images (3304×2336) is the HRF, having both healthy and diseased ones. The highest reported metrics in this dataset are *Se* of 0.8506 (Christodoulidis et al. [73]), *Sp* of 0.9868 (Kovacs et al. [62]), *Acc* of 0.9674 (Kovacs et al. [62]) and *AUC* of

0.9608 (Zhang et al. [64]). Most of the segmentation methods on HRF dataset have evaluated their performance by resizing the image to a much lower resolution thus reducing the computational overhead. But the drawback with resizing the images is, the thin vessel structures are masked out leaving behind only the larger vessels which are comparatively easier to segment. In contrast, Kovacs et al. [62] proposed a blind calibration technique than can be used to transform a trained model to different resolution datasets without compromising on accuracy. Their method is well suited for clinical scenarios where the images are acquired from various scanners and protocols.

Discussion

The need for computer-aided detection of retinal vessels has motivated the medical imaging community to develop better segmentation methods in the last two decades. Almost all the techniques from conventional image processing to sophisticated machine learning (including deep learning techniques) have been extensively explored. Most existing methods in the literature are quite successful in addressing issues like intensity inhomogeneity, CVR, segmentation of complex vessel structures (near bifurcation and crossover regions) and extraction of thin vessels. But still, there are some open and unsolved challenges which need to be addressed. Some of the open questions which needs to be addressed are:

- How does vessel segmentation method perform in the presence of abnormalities?
- How to design a method which can efficiently handle both major and minor vessel structures in retinal image?
- How to adopt the same approach on different images with various resolutions acquired across multiple imaging devices without downsampling to much lower resolutions?

These significant challenges have recently driven the retinal imaging community to tackle these issues. Most of the methods are designed to handle healthy images without accounting for abnormalities. The techniques in [31, 36, 78, 79] addressed, in particular, the problem of vessel segmentation in the presence of abnormalities. Most of the researchers evaluated their methods on DRIVE and STARE datasets although, a recent trend has moved towards CHASE_DB1 and HRF databases. A large number of images from these datasets is normal excluding ARIA and MESSIDOR. The number of images in these datasets is very limited ranging from 20 to 45 and are relatively easier to segment. From Table 1, it can be observed that only fewer methods evaluated their performance on ARIA and MESSIDOR although these datasets publicly released a long

Table 5 Comparison of segmentation methods on the DRIVE, STARE, CHASE_DB1 and HRF datasets

Methods	DRIVE			STARE			CHASE_DB1			HRF		
	Se	Sp	Acc	AUC	Se	Sp	Acc	AUC	Se	Sp	Acc	AUC
Supervised methods												
2nd human observer	0.7760	0.9724	0.9472	—	0.8952	0.9384	0.9349	—	0.8105	0.9711	0.9545	—
Fraz et al. [22]	0.7406	0.9807	0.9480	0.9747	0.7548	0.9763	0.9534	0.9768	0.7224	0.9711	0.9469	0.9712
Condurache et al. [46]	0.9094	0.9591	0.9516	0.9726	0.8902	0.9673	0.9595	0.9791	—	—	—	—
Fraz et al. [28]	—	—	—	—	—	—	—	—	0.7259	0.9770	0.9524	0.9760
Rahebi et al. [47]	0.7365	0.9707	0.9461	0.9564	0.6902	0.9804	0.9527	0.9462	—	—	—	—
Fathi et al. [48]	0.7649	—	0.9449	—	0.7505	—	0.9460	—	—	—	—	—
Ganjee et al. [49]	—	—	—	—	0.7437	—	0.9542	—	—	—	—	—
Orlando et al. [50]	0.7760	0.9730	—	0.9507	0.8951	0.9387	—	—	0.7277	0.9712	—	0.9359
Wang et al. [54]	0.8173	0.9733	0.9767	0.9475	0.8104	0.9791	0.9813	0.9751	—	—	—	—
Vega et al. [41]	0.7444	0.9600	0.9412	—	0.7019	0.9671	0.9483	—	—	—	—	—
Dai et al. [52]	0.7359	0.9720	0.9418	—	0.7769	0.9550	0.9364	—	—	—	—	—
Roychowdhury et al. [53]	0.7250	0.9830	0.9520	0.9620	0.7720	0.9730	0.9510	0.9690	—	—	—	—
Zhang et al. [71]	0.7812	0.9668	0.9504	—	—	—	—	—	—	—	—	—
Li et al. [55]	0.7569	0.9816	0.9527	0.9738	0.7726	0.9844	0.9628	0.9879	0.7507	0.9793	0.9581	0.9716
Liskowski et al. [56]	0.7811	0.9807	0.9535	0.9790	0.9289	0.9710	0.9667	0.9930	0.8793	0.9668	0.9577	0.9845
Fu et al. [59]	0.7294	—	0.9470	—	0.7140	—	0.9545	—	—	—	—	—
Strisciuglio et al. [60]	0.7777	0.9702	0.9454	0.9597	0.8046	0.9710	0.9534	0.9638	—	—	—	—
Abbasi et al. [101]	0.7695	0.9742	0.9477	0.9525	—	—	—	—	—	—	—	—
Unsupervised methods												
Wang et al. [44]	—	—	0.9461	0.9543	—	—	0.9521	0.9682	—	—	—	—
Azzopardi et al. [23]	0.7655	0.9704	0.9442	0.9614	0.7716	0.9701	0.9497	0.9563	0.7585	0.9587	0.9387	0.9487
Kovaes et al. [62]	0.7450	0.9793	0.9494	0.9722	0.8034	0.9786	0.9610	0.9836	—	—	—	0.7502
Kar et al. [63]	0.7548	0.9792	0.9616	—	0.7577	0.9788	0.9730	—	—	—	—	—
Zhang et al. [64]	0.7743	0.9725	0.9476	0.9636	0.7791	0.9758	0.9554	0.9748	0.7626	0.9661	0.9452	0.9606
Yu et al. [65]	0.7233	—	0.9426	—	0.7112	—	0.9463	—	—	—	—	0.7938
Moghmirad et al. [66]	0.7852	—	0.9659	0.9580	0.8133	—	0.9756	0.9678	—	—	—	—
Budai et al. [68]	0.6440	0.9870	0.9572	—	0.5800	0.9820	0.9386	—	—	—	—	0.6690
Nguyen et al. [24]	—	—	0.9407	—	—	—	0.9324	—	—	—	—	—
Fathi et al. [38]	0.7768	0.9759	0.9581	0.9516	0.8061	0.9717	0.9591	0.9680	—	—	—	—
Anunziata et al. [69]	—	—	—	—	0.7128	0.9836	0.9562	0.9655	—	—	—	0.7128
Abdallah et al. [70]	0.5879	—	0.9155	—	0.6145	—	0.9402	—	—	—	—	—
Yin et al. [72]	0.8957	—	0.9506	—	0.8886	—	0.9315	—	—	—	—	—

Table 5 (continued)

Methods	DRIVE			STARE			CHASE_DBI			HRF							
	Se	Sp	Acc	AUC	Se	Sp	Acc	AUC	Se	Sp	Acc	AUC	Se	Sp	Acc	AUC	
Christodoulidis et al. [73]	—	—	—	—	—	—	—	—	—	—	—	—	—	0.8506	0.9582	0.9479	—
Yin et al. [75]	0.6522	0.9710	0.9267	—	0.7248	0.9666	0.9412	—	—	—	—	—	—	—	—	—	—
Fraz et al. [43]	0.7152	0.9759	0.9430	—	0.7311	0.9680	0.9442	—	—	—	—	—	—	—	—	—	—
Fraz et al. [79]	0.7302	0.9742	0.9422	—	0.7318	0.9660	0.9423	—	—	—	—	—	—	—	—	—	—
Imani et al. [80]	0.7524	0.9753	0.9523	—	0.7502	0.9745	0.9590	—	—	—	—	—	—	—	—	—	—
Roychowdhury et al. [42]	0.7395	0.9782	0.9494	0.9672	0.7317	0.9842	0.9560	0.9673	0.7615	0.9575	0.9467	0.9623	—	—	—	—	—
Mapayi et al. [81]	0.7632	0.9634	0.9461	0.9658	0.7626	0.9657	0.9510	0.9781	—	—	—	—	—	—	—	—	—
Mapayi et al. [82]	0.7391	0.9569	0.9377	—	0.5031	0.9567	0.9221	—	—	—	—	—	—	—	—	—	—
Xiao et al. [83]	0.7513	0.9792	0.9529	—	0.7147	0.9735	0.9476	—	—	—	—	—	—	—	—	—	—
Gonzalez et al. [84]	0.7512	—	0.9412	—	0.7887	—	0.9441	—	—	—	—	—	—	—	—	—	—
Zhao et al. [25]	0.7354	0.9789	0.9477	—	0.7187	0.9767	0.9509	—	—	—	—	—	—	—	—	—	—
Zhao et al. [6]	0.7440	0.9780	0.9530	0.8610	0.7860	0.9750	0.9510	0.8810	—	—	—	—	—	—	—	—	—
Zhao et al. [40]	0.7420	0.9820	0.9540	0.8620	0.7800	0.9780	0.9560	0.8740	—	—	—	—	—	—	—	—	—
Hassanien et al. [86]	0.7210	0.9710	0.9388	—	0.6490	0.9820	0.9467	—	—	—	—	—	—	—	—	—	—
Frucci et al. [87]	0.6700	0.9860	0.9590	—	—	—	—	—	—	—	—	—	—	—	—	—	—
Lazar et al. [85]	0.7646	—	0.9458	—	0.7248	—	0.9492	—	0.7102	—	0.9533	—	—	—	—	—	—

time ago. Further, a large number of existing methods are evaluated on the retinal images of adults. The morphological attributes of retinal images of premature infants and children's are entirely different than that of adults. The choroidal vessels, CVR, and other illumination artefacts are more prominently visible in young individuals than the older population [28]. Hence, there is a further scope for developing newer segmentation methods that performs well for both adult as well as paediatric retinal images.

The existing methods in the literature are mainly focused on segmenting large vessel structures leaving behind the thin and low contrast vessels. To the best of our knowledge, only a few number of existing studies have addressed the segmentation of thin vessels in fundus images. In this regard, methods in [25, 42, 52, 55, 64, 73] have made an attempt to specifically address the problem of thin vessel segmentation. Among these methods, the method in [73] has achieved a significant state-of-the-art results compared to previous methods for segmentation of thin vessels. But still there exists difficulty in segmenting vessels which lies at extremely low contrast and junction locations. In addition, "the performance assessment of the existing methods is solely based on global classification metric which does not take into account the fact that the smallest vessels represent approximately 10 % of the total surface area of the vascular network" [73].

Current segmentation methods are mainly evaluated on color fundus images. Most of these images are often corrupted by noise, blur, and non-uniform illumination. Hence, it is often difficult for accurate segmentation of thin and low contrast vessel structures. The advancements in newer retinal imaging modalities (like FA, SLO, OCT) and with the integration of adaptive optics [106] to these modalities has provided a better spatial as well as transverse resolution. These newer imaging modalities provide better visualization of vessels and other micro-structures. Further, this opens new research direction in better understanding the structural and physiological changes that affect the retinal vasculature. Some of the newer methods like [64, 96, 101] have made an attempt to evaluate the segmentation performance on FA and SLO images. Further, this provides an opportunity for the researchers to validate their technique on high resolution, high contrast, and finely detailed images.

Conclusions

In this paper, we presented a comprehensive review of recent state-of-the-art retinal vessel segmentation methods published in the last five years. The various complexities and challenges involved in developing robust segmentation techniques have been discussed including the most crucial image preprocessing steps that have not been addressed

earlier in the literature. In addition, the strengths and weakness of each category of segmentation methods with focus to current challenges are discussed in detail. Further, an in-depth quantitative evaluation of state-of-the-art approaches on the individual dataset is assessed. Although many articles have been published on the automated segmentation of retinal vessels, still there exists room for further improvements. Most of the previous methods have dealt with the fewer images mostly healthier ones, typically segmenting the larger vessel structures and much lower resolution input images. Thus, some of the challenges that remain open to the research community are segmentation in the presence of abnormalities, accurate segmentation of thin vessel structures and segmentation in the presence of non-uniform illumination and various other imaging artefacts.

Acknowledgments The authors gratefully acknowledge Prof. Jayanthi Sivaswamy (CVIT, IIT-Hyderabad), Samrudhhi Rangrej, Sukanya Kudi, Raghav Mehta (CVIT, IIT-Hyderabad) and Praveen GB (BITS-Goa) for the fruitful discussions and valuable suggestions in improving the paper.

Compliance with Ethical Standards

Conflict of interests All authors declares that he/she has no conflict of interest.

Ethical approval This article does not contain any studies with human participants or animals performed by any of the authors.

References

1. Yau, J. W. Y., and et al., Global prevalence and major risk factors of diabetic retinopathy. *Diabetes Care* 35.3:556–564, 2012.
2. Wong, W. L., and et al., xGlobal prevalence of age-related macular degeneration and disease burden projection for 2020 and 2040: a systematic review and meta-analysis. *The Lancet Global Health* 2.2:e106–e116, 2014.
3. Tham, Y.-C., and et al., Global prevalence of glaucoma and projections of glaucoma burden through 2040: a systematic review and meta-analysis. *Ophthalmology* 121.11:2081–2090, 2014.
4. Abramoff, M. D., Garvin, M. K., and Sonka, M., Retinal imaging and image analysis. *IEEE Rev. Biomed. Eng.* 3:169–208, 2010.
5. Fraz, M. M., and et al., Blood vessel segmentation methodologies in retinal images—a survey. *Comput. Methods Prog. Biomed.* 108.1:407–433, 2012.
6. Zhao, Y., and et al., Retinal vessel segmentation: An efficient graph cut approach with retinex and local phase. *PLoS One* 10.4:e0122332, 2015.
7. Wong, T. Y., and et al., Retinal microvascular changes and MRI signs of cerebral atrophy in healthy, middle-aged people. *Neurology* 61.6:806–811, 2003.
8. Doubal, F. N., Hokke, P. E., and Wardlaw, J. M., Retinal microvascular abnormalities and stroke: a systematic review. *J. Neurol. Neurosurg. Psychiatry* 80.2:158–165, 2009.
9. Smith, W., and et al., Retinal arteriolar narrowing is associated with 5-year incident severe hypertension the Blue Mountains Eye Study. *Hypertension* 44.4:442–447, 2004.

10. Wong, T. Y., and et al., Retinal microvascular abnormalities and their relationship with hypertension, cardiovascular disease, and mortality. *Surv. Ophthalmol.* 46.1:59–80, 2001.
11. Wong, T., and Mitchell, P., The eye in hypertension. *Lancet* 369.9559:425–435, 2007.
12. Wong, T. Y., and et al., Retinal microvascular abnormalities and incident stroke: the Atherosclerosis Risk in Communities Study. *Lancet* 358.9288:1134–1140, 2001.
13. Sharrett, A., and et al., Richey Retinal arteriolar diameters and elevated blood pressure the atherosclerosis risk in communities study. *Am. J. Epidemiol.* 150.3:263–270, 1999.
14. Tso, M. O. M., and Jampol, L. M., Pathophysiology of hypertensive retinopathy. *Ophthalmology* 89.10:1132–1145, 1982.
15. Hoover, A., and Goldbaum, M., Locating the optic nerve in a retinal image using the fuzzy convergence of the blood vessels. *IEEE Trans. Med. Imaging* 22.8:951–958, 2003.
16. Welikala, R. A., and et al., Automated detection of proliferative diabetic retinopathy using a modified line operator and dual classification. *Comput. Methods Prog. Biomed.* 114.3:247–261, 2014.
17. Cheung, C. S. Y., and et al., Computer-assisted image analysis of temporal retinal vessel width and tortuosity in retinopathy of prematurity for the assessment of disease severity and treatment outcome. *J. Am. Assoc. Pediatr. Ophthalmol. Strabismus* 15.4:374–380, 2011.
18. Sutter, F. K. P., and Helbig, H., Familial retinal arteriolar tortuosity: a review. *Surv. Ophthalmol.* 48.3:245–255, 2003.
19. Grisan, E., Foracchia, M., and Ruggeri, A., A novel method for the automatic grading of retinal vessel tortuosity. *IEEE Trans. Med. Imaging* 27.3:310–319, 2008.
20. Sodi, A., and et al., Computer assisted evaluation of retinal vessels tortuosity in Fabry disease. *Acta Ophthalmol.* 91.2:e113–e119, 2013.
21. Marín, D., and et al., A new supervised method for blood vessel segmentation in retinal images by using gray-level and moment invariants-based features. *IEEE Trans. Med. Imaging* 30.1:146–158, 2011.
22. Fraz, M. M., and et al., An ensemble classification-based approach applied to retinal blood vessel segmentation. *IEEE Trans. Biomed. Eng.* 59.9:2538–2548, 2012.
23. Azzopardi, G., and et al., Trainable COSFIRE filters for vessel delineation with application to retinal images. *Med. Image Anal.* 19.1:46–57, 2015.
24. Nguyen, U. T. V., and et al., An effective retinal blood vessel segmentation method using multi-scale line detection. *Pattern Recogn.* 46.3:703–715, 2013.
25. Zhao, Y. Q., and et al., Retinal vessels segmentation based on level set and region growing. *Pattern Recogn.* 47.7:2437–2446, 2014.
26. Mendonca, A. M., and Campilho, A., Segmentation of retinal blood vessels by combining the detection of centerlines and morphological reconstruction. *IEEE Trans. Med. Imaging* 25.9:1200–1213, 2006.
27. Narasimha-Iyer, H., and et al., Improved detection of the central reflex in retinal vessels using a generalized dual-Gaussian model and robust hypothesis testing. *IEEE Trans. Inf. Technol. Biomed.* 12.3:406–410, 2008.
28. Fraz, M. M., and et al., Delineation of blood vessels in pediatric retinal images using decision trees-based ensemble classification. *Int. J. Comput. Assist. Radiol. Surg.* 9.5:795–811, 2014.
29. Ricci, E., and Perfetti, R., Retinal blood vessel segmentation using line operators and support vector classification. *IEEE Trans. Med. Imaging* 26.10:1357–1365, 2007.
30. Azzopardi, G., and Petkov, N., Automatic detection of vascular bifurcations in segmented retinal images using trainable COSFIRE filters. *Pattern Recogn. Lett.* 34.8:922–933, 2013.
31. Sigursson, E. M., and et al., Automatic retinal vessel extraction based on directional mathematical morphology and fuzzy classification. *Pattern Recogn. Lett.* 47:164–171, 2014.
32. Fraz, M. M., and et al., Quantification of blood vessel calibre in retinal images of multi-ethnic school children using a model based approach. *Comput. Med. Imaging Graph.* 37.1:48–60, 2013.
33. Chaudhuri, S., and et al., Detection of blood vessels in retinal images using two-dimensional matched filters. *IEEE Trans. Med. Imaging* 8.3:263–269, 1989.
34. Gang, L., Chutatape, O., and Krishnan, S. M., Detection and measurement of retinal vessels in fundus images using amplitude modified second-order Gaussian filter. *IEEE Trans. Biomed. Eng.* 49.2:168–172, 2002.
35. Frangi, A. F., and et al.: Multiscale vessel enhancement filtering. International Conference on Medical Image Computing and Computer-Assisted Intervention Springer Berlin Heidelberg, 1998.
36. Palomera-Pérez, M. A., and et al., Parallel multiscale feature extraction and region growing: application in retinal blood vessel detection. *IEEE Trans. Inf. Technol. Biomed.* 14.2:500–506, 2010.
37. Bankhead, P., and et al., Fast retinal vessel detection and measurement using wavelets and edge location refinement. *PLoS One* 7.3:e32435, 2012.
38. Fathi, A., and Naghsh-Nilchi, A. R., Automatic wavelet-based retinal blood vessels segmentation and vessel diameter estimation. *Biomed. Signal Process. Control* 8.1:71–80, 2013.
39. Soares, J. V. B., and et al., Retinal vessel segmentation using the 2-D Gabor wavelet and supervised classification. *IEEE Trans. Med. Imaging* 25.9:1214–1222, 2006.
40. Zhao, Y., and et al., Automated vessel segmentation using infinite perimeter active contour model with hybrid region information with application to retinal images. *IEEE Trans. Med. Imaging* 34.9:1797–1807, 2015.
41. Vega, R., and et al., Retinal vessel extraction using lattice neural networks with dendritic processing. *Comput. Biol. Med.* 58:20–30, 2015.
42. Roychowdhury, S., Koozekanani, D. D., and Parhi, K. K., Iterative vessel segmentation of fundus images. *IEEE Trans. Biomed. Eng.* 62.7:1738–1749, 2015.
43. Fraz, M. M., and et al., An approach to localize the retinal blood vessels using bit planes and centerline detection. *Comput. Methods Prog. Biomed.* 108.2:600–616, 2012.
44. Wang, Y., and et al., Retinal vessel segmentation using multi-wavelet kernels and multiscale hierarchical decomposition. *Pattern Recogn.* 46.8:2117–2133, 2013.
45. Youssef, D., and Solouma, N. H., Accurate detection of blood vessels improves the detection of exudates in color fundus images. *Comput. Methods Prog. Biomed.* 108.3:1052–1061, 2012.
46. Condurache, A. P., and Mertins, A., Segmentation of retinal vessels with a hysteresis binary-classification paradigm. *Comput. Med. Imaging Graph.* 36.4:325–335, 2012.
47. Rahebi, J., and Frat, H., Retinal blood vessel segmentation with neural network by using gray-level co-occurrence matrix-based features. *J. Med. Syst.* 38.8:1–12, 2014.
48. Fathi, A., and Naghsh-Nilchi, A. R., General rotation-invariant local binary patterns operator with application to blood vessel detection in retinal images. *Pattern. Anal. Applic.* 17.1:69–81, 2014.
49. Ganjee, R., Azmi, R., and Gholizadeh, B., An improved retinal vessel segmentation method based on high level features for pathological images. *J. Med. Syst.* 38.9:1–9, 2014.

50. Orlando, J. I., Prokofyeva, E., and Blaschko, M. B., A discriminatively trained fully connected conditional random field model for blood vessel segmentation in fundus images. *IEEE Trans. Biomed. Eng.* 64.1:16–27, 2017.
51. Cheung, C. Y.-L., and et al., Microvascular network alterations in the retina of patients with Alzheimer's disease. *Alzheimers Dement.* 10.2:135–142, 2014.
52. Dai, P., and et al., A new approach to segment both main and peripheral retinal vessels based on gray-voting and gaussian mixture model. *PLoS One* 10.6:e0127748, 2015.
53. Roychowdhury, S., Koozekanani, D. D., and Parhi, K. K., Blood vessel segmentation of fundus images by major vessel extraction and subimage classification. *IEEE J. Biomed. Health Inform.* 19.3:1118–1128, 2015.
54. Wang, S., and et al., Hierarchical retinal blood vessel segmentation based on feature and ensemble learning. *Neurocomputing* 149:708–717, 2015.
55. Li, Q., and et al., A Cross-Modality Learning Approach for Vessel Segmentation in Retinal Images. *IEEE Trans. Med. Imaging* 35.1:109–118, 2016.
56. Liskowski, P., and Krawiec, K., Segmenting Retinal Blood Vessels with Deep Neural Networks. *IEEE Trans. Med. Imaging* 35.11:2369–2380, 2016.
57. Maninis, K.-K., and et al.: Deep retinal image understanding. International Conference on Medical Image Computing and Computer-Assisted Intervention Springer International Publishing, 2016.
58. Wu, A., and et al.: Deep vessel tracking: A generalized probabilistic approach via deep learning. Biomedical Imaging (ISBI), 2016 IEEE 13th International Symposium on IEEE, 2016.
59. Fu, H., Xu, Y., Wong, D. W. K., and Liu, J.: Retinal vessel segmentation via deep learning network and fully-connected conditional random fields, 2016 IEEE 13th International Symposium on Biomedical Imaging (ISBI), Prague, 698–701, 2016.
60. Strisciuglio, N., and et al.: Supervised vessel delineation in retinal fundus images with the automatic selection of B-COSFIRE filters. *Machine Vision and Applications*, 1–13, 2016.
61. Krause, M., and et al., Fast retinal vessel analysis. *J. Real-Time Image Proc.* 11.2:413–422, 2016.
62. Kovács, G., and András, H., A self-calibrating approach for the segmentation of retinal vessels by template matching and contour reconstruction. *Med. Image Anal.* 29:24–46, 2016.
63. Kar, S. S., and Maity, S. P., Blood vessel extraction and optic disc removal using curvelet transform and kernel fuzzy c-means. *Comput. Biol. Med.* 70:174–189, 2016.
64. Zhang, J., and et al.: Robust retinal vessel segmentation via locally adaptive derivative frames in orientation scores IEEE Transactions on Medical Imaging, 2016.
65. Yu, H., and et al.: Fast vessel segmentation in retinal images using multiscale enhancement and second-order local entropy. SPIE Medical Imaging International Society for Optics and Photonics, 2012.
66. Moghimirad, E., Rezatofghi, S. H., and Soltanian-Zadeh, H., Retinal vessel segmentation using a multi-scale medialness function. *Comput. Biol. Med.* 42.1:50–60, 2012.
67. Zheng, J., and et al.: Retinal image graph-cut segmentation algorithm using multiscale hessian-enhancement-based nonlocal mean filter. *Computational and Mathematical Methods in Medicine* 2013, 2013.
68. Budai, A., and et al.: Robust vessel segmentation in fundus images. *International Journal of Biomedical Imaging* 2013, 2013.
69. Annunziata, R., and et al., Leveraging multiscale hessian-based enhancement with a novel exudate inpainting technique for retinal vessel segmentation. *IEEE J. Biomed. Health Inform.* 20.4:1129–1138, 2016.
70. Abdallah, M. B., and et al.: Automatic extraction of blood vessels in the retinal vascular tree using multiscale medialness. *Journal of Biomedical Imaging* 2015, 2015.
71. Zhang, L., Fisher, M., and Wang, W., Retinal vessel segmentation using multi-scale textons derived from keypoints. *Comput. Med. Imaging Graph.* 45:47–56, 2015.
72. Yin, B., and et al., Vessel extraction from non-fluorescein fundus images using orientation-aware detector. *Med. Image Anal.* 26.1:232–242, 2015.
73. Christodoulidis, A., and et al.: A Multi-scale Tensor Voting Approach for Small Retinal Vessel Segmentation in High Resolution Fundus Images Computerized Medical Imaging and Graphics, 2016.
74. Yin, Y., Adel, M., and Bourennane, S., Retinal vessel segmentation using a probabilistic tracking method. *Pattern Recogn.* 45.4:1235–1244, 2012.
75. Yin, Y., Adel, M., and Bourennane, S.: Automatic segmentation and measurement of vasculature in retinal fundus images using probabilistic formulation. *Computational and Mathematical Methods in Medicine* 2013, 2013.
76. Zhang, J., and et al., A retinal vessel boundary tracking method based on Bayesian theory and multi-scale line detection. *Comput. Med. Imaging Graph.* 38.6:517–525, 2014.
77. De, J., Li, H., and Li, C., Tracing retinal vessel trees by transductive inference. *BMC Bioinf.* 15:1, 2014.
78. Bekkers, E., and et al., A multi-orientation analysis approach to retinal vessel tracking. *J. Math. Imaging Vision* 49.3:583–610, 2014.
79. Fraz, M. M., Basit, A., and Barman, S. A., Application of morphological bit planes in retinal blood vessel extraction. *J. Digit. Imaging* 26.2:274–286, 2013.
80. Imani, E., Javidi, M., and Pourreza, H.-R., Improvement of retinal blood vessel detection using morphological component analysis. *Comput. Methods Prog. Biomed.* 118.3:263–279, 2015.
81. Mapayi, T., Viriri, S., and Tapamo, J.-R.: Adaptive Thresholding Technique for Retinal Vessel Segmentation Based on GLCM-Energy Information. *Computational and Mathematical Methods in Medicine* 2015, 2015.
82. Mapayi, T., Viriri, S., and Tapamo, J.-R.: Comparative Study of Retinal Vessel Segmentation Based on Global Thresholding Techniques. *Computational and Mathematical Methods in Medicine* 2015, 2015.
83. Xiao, Z., Adel, M., and Bourennane, S.: Bayesian method with spatial constraint for retinal vessel segmentation. *Computational and Mathematical Methods in Medicine* 2013, 2013.
84. Salazar-Gonzalez, A., and et al., Segmentation of blood vessels and optic disc in retinal images. *IEEE J. Biomed. Health Inform.* 2194:1–1, 2014.
85. Lazar, I., and Hajdu, A., Segmentation of retinal vessels by means of directional response vector similarity and region growing. *Comput. Biol. Med.* 66:209–221, 2015.
86. Hassanien, A. E., Emary, E., and Zawbaa, H. M., Retinal blood vessel localization approach based on bee colony swarm optimization, fuzzy c-means and pattern search. *J. Vis. Commun. Image Represent.* 31:186–196, 2015.
87. Frucci, M., and et al.: Severe: Segmenting vessels in retina images. *Pattern Recognition Letters*, 2015.
88. DRIVE: digital retinal images for vessel extraction, <http://www.isi.uu.nl/Research/Databases/DRIVE>, 2004.

89. Hoover, A. D., Kouznetsova, V., and Goldbaum, M., Locating blood vessels in retinal images by piecewise threshold probing of a matched filter response. *IEEE Trans. Med. Imaging* 19.3:203–210, 2000.
90. ARIA Online, Retinal Image Archive, <http://www.eyecharity.com/ariaonline/>, 2006.
91. Odstrcilik, J., and et al., Retinal vessel segmentation by improved matched filtering: evaluation on a new high-resolution fundus image database. *IET Image Process.* 7.4:373–383, 2013.
92. Klviinen, R., Voutilainen², J., Pietil⁴, H., and Uusitalo, H., DIARETDB1 diabetic retinopathy database and evaluation protocol. *Med. Image Understanding Anal.* 2007:61, 2007.
93. MESSIDOR: Methods for Evaluating Segmentation and Indexing Techniques Dedicated to Retinal Ophthalmology, <http://messidor.crihan.fr/index-en.php>, 2004.
94. Al-Diri, B., and et al.: REVIEW-a reference data set for retinal vessel profiles. 2008 30th Annual International Conference of the IEEE Engineering in Medicine and Biology Society IEEE, 2008.
95. Pitzer, S. M., Adaptive histogram equalization and its variations. *Comp. Vision Graph. Image Pros.* 39:355–368, 1987.
96. Perez-Rovira, A., and et al.: Improving vessel segmentation in ultra-wide field-of-view retinal fluorescein angiograms. 2011 Annual International Conference of the IEEE Engineering in Medicine and Biology Society IEEE, 2011.
97. IOSTAR dataset. [Online]. Available: www.retinacheck.org, 2015.
98. RC-SLO dataset. [Online]. Available: www.retinacheck.org, 2015.
99. Gegúndez-Arias, M. E., and et al., A function for quality evaluation of retinal vessel segmentations. *IEEE Trans. Med. Imaging* 31.2:231–239, 2012.
100. Alipour, S. H. M., Hossein, R., and Mohammadreza, A., A new combined method based on curvelet transform and morphological operators for automatic detection of foveal avascular zone. *SIViP* 8.2:205–222, 2014.
101. Abbasi-Sureshjani, S., and et al.: Biologically-inspired supervised vasculature segmentation in SLO retinal fundus images. International Conference Image Analysis and Recognition Springer International Publishing, 2015.
102. Nguyen, U. T. V., and et al., An automated method for retinal arteriovenous nicking quantification from color fundus images. *IEEE Trans. Biomed. Eng.* 60.11:3194–3203, 2013.
103. Oloumi, F., and et al., Computer-aided diagnosis of plus disease via measurement of vessel thickness in retinal fundus images of preterm infants. *Comput. Biol. Med.* 66:316–329, 2015.
104. Staal, J., and et al., Ridge-based vessel segmentation in color images of the retina. *IEEE Trans. Med. Imaging* 23.4:501–509, 2004.
105. Foracchia, M., Grisan, E., and Ruggeri, A., Luminosity and contrast normalization in retinal images. *Med. Image Anal.* 9.3:179–190, 2005.
106. Felberer, F., and et al., Imaging of retinal vasculature using adaptive optics SLO/OCT. *Biomed. Opt. Express* 6.4:1407–1418, 2015.